EFFECTS OF THERMAL RADIATION AND BUOYANCY FORCE ON TRANSIENT HARTMANN FLOW IN A CHANNEL WITH PERMEABLE WALLS

O. PRAKASH† and O.D. MAKINDE‡

† *School of Basic and Applied Sciences, Galgotias University Greater Noida, Uttar Pradesh, India*
Corresponding author: op_ibs@rediffmail.com
‡ *Faculty of Military Science, Stellenbosch University Private Bag X2, Saldanha 7395, South Africa.*

***Abstract*— In this paper the combined effects of thermal radiation, buoyancy force and variable heat source on an unsteady MHD flow of a conducting fluid through a porous walled channel has been theoretically investigated. Base on some simplified assumptions, the model partial differential equations are obtained and tackled analytically using variable separable techniques and numerically via Runge-Kutta-Fehlberg integration scheme. Pertinent results depicting the impact of various embedded thermo-physical parameters on the fluid velocity, temperature profiles, skin friction and Nusselt number are displayed graphically and discussed quantitatively. An escalation in both skin friction and heat transfer rate is observed with a rise in fluid injection–suction at the channel walls.**

***Keywords*— Unsteady flow; Permeable channel; Buoyancy force; Radiative heat.**

I. INTRODUCTION

Studies related to thermal radiation interaction with hydro-magnetic mixed convection in a channel with permeable walls have been of great interest to many researchers due to its vast uses in physiological flow processes and engineering. Magneto-hydrodynamics is also vastly useful and used in distinct magnetic drug targeting like cancer diseases. Meanwhile, blood is a bio-magnetic fluid and its flows can be affected by the existence of a magnetic field due to the complex interaction of the intercellular protein. Arterial walls are bounded by tissues and are idealized as permeable surface through which blood nutrient are supply into the surrounding tissues (Prakash *et al.*, 2015a; Ramakrishnan and Shailendhra, 2013). The application of thermal radiation therapy to human body can increase the resilience of ligaments and tendons alleviate pain, decreases muscle contractions, elevate blood flow and boost metabolism. Heat plays an important role in rebuild the tissue by increasing blood flow and repair of tissue (Nadler *et al*., 2004). Enhanced blood circulation falls in heated parts of the body due to heat inclines to loosen up the walls of blood artery. Furthermore, hydro-magnetic mixed convection with thermal radiation in porous channel is also useful in various engineering problems like electromagnetic casting, nuclear reactors, and plasma confinement. In a pioneering work, Hartmann and Lazarus (1937) investigated the impact of uniform magnetic field on the flow of a conducting fluid between two too long plates. Thereafter, numerous similar efforts have been carried out by many researchers under different physical conditions (Cramer and Pai, 1973; Das *et al*., 2015). Ramamurthy and Shanker (1994) discussed magneto-hydrodynamic impacts on blood flow in presence of porous medium. Yang and Yu (1974) numerically analyzed the flow of convective MHD flow between two parallel plates treated with concurrently in presence of pressure gradient and an axial temperature gradient. It has been discovered that an applied transverse magnetic field reasonably decreases the entrance length of the velocity, but it is a small influence can be seen on the temperature development. Malton and Schweitzer (1974) considered the model of a liquid conductor limited between two concentric cylindrical electrodes which were derived by electromagnetic. Tzirtzilakis (2005) studied MHD third grade blood flow in a stenosed artery to obtain the flow characteristics like the volume flow rate, flow velocity, resistance to the flow and the shear stress. Ansari *et al*. (2011) analyzed the unsteady MHD flow of a viscous fluid in a moving channel with finitely conducting plates, inspired because of an oscillating pressure gradient, in the appearance of a constant magnetic field. The effect of viscosity and thermal conductivity with heat transfer on the Hartmann flow with assumption that viscosity is dependent on temperature discussed by Attia and Hassan (2003). Makinde and Onyejekwe (2011) proposed a model for a numerical study of MHD generalized Couette flow and heat transfer in presence of electrical conductivity and variable viscosity. Hussam and Sheard (2013) investigated MHD duct flow in presence of heat transfer with a high Hartmann number in a circular cylinder. Adhikary and Misra (2011) worked on heat transfer on unsteady two-dimensional hydro-magnetic flow. Meanwhile, MHD mixed convection may be characterized as heat transfer situations where pressure, magnetic field and buoyancy forces merged. In vertical channels, the bulk fluid flow can flow either upward or downward direction, and thermal buoyancy forces may be either opposing or assisting the forced flow. In the literature, problems related to buoyancy assisted flow considered by some authors (Makinde and Chinyoka, 2010; Babu *et al*., 2018) induced heat in upward flows or cooling on downward flows. In this case, the axial velocities may enhance near the channel plates due to temporal or spatial variation in the wall temperature and reduce within the main region, with chances of existence of a flow recirculation in the channel (Gau *et al*., 1992). The effects of viscous dissipation, ohmic-viscous dissipation and suction/injection on MHD flow of a nanofluid over different channels in the presence of porous medium were analyzed by Pandey and Kumar (2016), Pandey and Kumar (2017) and Upreti *et al*. (2018a). Upreti *et al*. (2020a) discussed the impacts of non-uniform heat source/sink and Ohmic heating on 3D magneto hydrodynamic flow of water–CNTs (SWCNT and MWCNT) nanofluid. Upreti *et al.* (2020b) proposed a model to discuss the effects of heat and mass transfer flow of Ag–kerosene oil nanofluid under applied magnetic field and Ohmic-viscous dissipation.

Moreover, the effect of radiative heat transfer is extremely important for philological and engineering flow process operating at high temperature (Brewster, 1992). Thermal radiation refers to the emission of a spectrum of electromagnetic radiation due to the temperature of the material (Makinde and Ogulu, 2008; Ozisik, 1973; Rosseland, 1936). Thermal radiation consistently present and can firmly merge with convection in many circumstances. Practical applications of the mixed convection in the presence of thermal radiation include; deep heat muscle treatment physiotherapy, combustion chambers, cooling towers and rocket engines and solar collectors. Prakash and Makinde (2011) studied the influence of radiative heat transfer on hydro-magnetic blood flow in a stenotic artery in the presence of erythrocytes. Govindarajan and Sahu (2011) proposed a model for two fluid channel flow of a system and found a new double-diffusive mode of instability. Das *et al*. (2014) analyzed experimentally described the collective normal modes of dusty plasma medium and consider non linear dynamics characteristics features. Recently, Prakash *et al.* (2015b) presented a model on MHD oscillatory flow of dusty fluid in a channel filled with a porous medium. The validity of Magnetic Reynolds Number in the MHD fluid flow is analyzed by (Sarris *et al*., 2006; Khan *et al*., 2007; Glukhov and Sidorov, 2019; Zamzari *et al*., 2019).

In this current study, our aim is to carry on the earlier work of Ramakrishnan and Shailendhra (2013) and Prakash *et al.* (2015b) on hydro-magnetic flow passage through a uniform channel with permeable walls to include the amalgamate effects of buoyancy force, thermal radiation and flow unsteadiness. The physical motivation behind this study is based on bio-magnetic fluid dynamics that occur during deep heat muscle treatment physiotherapy. In the following section, the problem is formulated, solved, analyzed and discussed qualitatively.

II. MATHEMATICAL ANALYSIS

We propose unsteady flow of a thermally and electrically conducting viscous, incompressible, fluid between two infinite parallel permeable plates placed at $y = 0$ and $y = L$ in the presence of a uniform transverse magnetic field B_0 which is applied parallel to y-axis. It is considered that the flow is driven by the combined action of imposed pressure gradient and thermal buoyancy. In addition, fluid injection is applied at left plate of the channel while fluid suction present at the right plate. The left plate of channel is sustained at temperature T_0 while the right plate is maintained at temperature T_1 such that $T_0 \leq T_1$. Schematics diagram of the problem is given in Fig. 1.

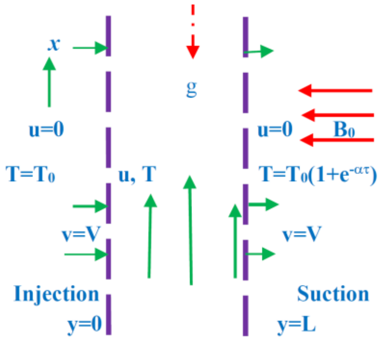

Figure 1: Schematic diagram of the problem

Considering the afore said assumptions, the mathematical equations using the Boussinesq approximation are written below (Prakash *et al.*, 2020, Makinde and Chinyoka, 2010)

$$\frac{\partial u}{\partial \tau} - V\frac{\partial u}{\partial y} = -\frac{1}{\rho}\frac{\partial p}{\partial x} + \upsilon\frac{\partial^2 u}{\partial y^2} - \frac{\sigma B_0^2 u}{\rho} + \beta g(T - T_0), \quad (1)$$

$$\rho c_p\left(\frac{\partial T}{\partial \tau} - V\frac{\partial T}{\partial y}\right) = k\frac{\partial^2 T}{\partial y^2} - \frac{\partial q_r}{\partial y} + Q(T - T_0). \quad (2)$$

Using the Rosseland approximation for thermal radiation in optically thick media, the radiative heat flux q_r is represented by Makinde and Chinyoka (2010), Babu *et al.* (2018), Gau *et al.* (1992), Brewster (1992), Makinde and Ogulu (2008) and Ozisik (1973).

$$q_r = -\frac{4\sigma^*}{3k^*}\frac{\partial T^4}{\partial y} \approx -\frac{16\sigma^* T_0^3}{3k^*}\frac{\partial T}{\partial y}, \quad (3)$$

where σ^* represents the Stefan–Boltzman constant and k^* denotes the mean absorption coefficient. The expression in Eq. (3) is obtained by considering that the temperature differences between the fluid and the channel plates are reasonable small and $T^4 \approx 4TT_0^3 - 3T_0^4$. The appropriate initial and boundary conditions for the temperature and fluid velocities are mentioned below:

$$u(y,0) = F(y),\ T(y,0) = H(y), \quad (4)$$
$$u(0,\tau) = 0,\ T(0,\tau) = T_0,$$
$$u(L,\tau) = 0,\ T(L,\tau) = T_0(1 + e^{-\alpha\tau}).$$

We establish the dimensionless variables as follows:

$$\eta = \frac{y}{L},\ X = \frac{x}{L},\ \theta = \frac{T - T_0}{T_0},\ t = \frac{\tau\upsilon}{L^2},\ \upsilon = \frac{\mu}{\rho},\ U = \frac{uL}{\upsilon}, \quad (5)$$
$$\lambda = \frac{\alpha L^2}{\upsilon},\ Nr = \frac{16\sigma^* T_0^3}{3kk^*},\ \mathrm{Re} = \frac{VL}{\upsilon},\ \mathrm{Pr} = \frac{\mu c_p}{k},\ M = \frac{\sigma B_0^2 L^2}{\mu},$$
$$\bar{P} = \frac{L^2 P}{\rho\upsilon^2},\ Gr = \frac{\beta g T_0 L^3}{\upsilon^2},\ S = \frac{QL^2}{\rho c_p \upsilon}.$$

Substituting Eq. (5) into Eqs. (1)-(4), we obtain,

$$\frac{\partial U}{\partial t} - \mathrm{Re}\frac{\partial U}{\partial \eta} = -\frac{\partial \bar{P}}{\partial X} + \frac{\partial^2 U}{\partial \eta^2} - MU + Gr\theta, \quad (6)$$

$$\frac{\partial \theta}{\partial t} - \mathrm{Re}\frac{\partial \theta}{\partial \eta} = \left(\frac{1 + Nr}{\mathrm{Pr}}\right)\frac{\partial^2 \theta}{\partial \eta^2} + S\theta, \quad (7)$$

$$U(\eta,0) = F(\eta),\ \theta(\eta,0) = H(\eta), \quad (8)$$
$$U(0,t) = 0,\ U(1,t) = 0,\ \theta(L,t) = 0,\ \theta(1,t) = e^{-\lambda t}.$$

Skin friction coefficients (Cf) and Nusselt number (Nu) are given as

$$Cf = \frac{L^2\tau_w}{\rho\upsilon^2} = \frac{dU}{d\eta}\Big|_{\eta=0,1},\ Nu = -\frac{Lq_m}{kT_0} = \frac{d\theta}{d\eta}\Big|_{\eta=0,1}, \quad (9)$$

where

$$\tau_w = \mu\frac{\partial u}{\partial y},\ q_m = -k\frac{\partial T}{\partial y}. \quad (10)$$

III. METHOD OF SOLUTION

For the solution of Eqs. (6)-(8) analytically, we employ separation of variable technique, Prakash *et al.* (2020). For that, we assume:

$$-\frac{\partial \bar{p}}{\partial x} = Ae^{-\lambda t}, U(\eta,t) = F(\eta)e^{-\lambda t}, \theta(\eta,t) = H(\eta)e^{-\lambda t}, \quad (11)$$

Equation (11) depicts that the flow and temperature fields are driven by a time dependent exponentially decreasing pressure gradient. On solving the Eqs. (6), (7), (8) and (11), we obtain

$$\frac{\partial^2 F}{\partial \eta^2} + \mathrm{Re}\frac{\partial F}{\partial \eta} + (\lambda - M)F = -A - GrH, \quad (12)$$

$$\left(\frac{1+Nr}{\mathrm{Pr}}\right)\frac{\partial^2 H}{\partial \eta^2} + \mathrm{Re}\frac{\partial H}{\partial \eta} + (\lambda + S)H = 0, \quad (13)$$

The boundary conditions reduce to

$$F(0) = 0, H(0) = 0, \quad (14)$$
$$F(1) = 0, H(1) = 1.$$

Equations (12)-(14) are tackled analytically and we obtained the following solutions for the velocity and temperature profiles:

$$U(\eta,t) = (k_1e^{m_1\eta} + k_2e^{-m_2\eta} + k_3e^{m_3\eta} + k_4e^{-m_4\eta} - \frac{A}{c})e^{-\lambda t}, \quad (15)$$

$$\theta(\eta,t) = \left(\frac{e^{m_1\eta} - e^{-m_2\eta}}{n_1}\right)e^{-\lambda t}, \quad (16)$$

where

$$a = \frac{1+Nr}{\mathrm{Pr}}, b = \lambda + S, c = \lambda - M, \quad (17)$$

$$m_1 = \frac{-\mathrm{Re}+\sqrt{\mathrm{Re}^2-4ab}}{2a}, m_2 = \frac{\mathrm{Re}+\sqrt{\mathrm{Re}^2-4ab}}{2a}, n_1 = e^{m_1} - e^{-m_2},$$

$$m_3 = \frac{-\mathrm{Re}+\sqrt{\mathrm{Re}^2-4c}}{2}, m_4 = \frac{\mathrm{Re}+\sqrt{\mathrm{Re}^2-4c}}{2},$$

$$k_1 = -\frac{Gr}{n_1(m_1^2+\mathrm{Re}m_1+c)}, k_2 = \frac{Gr}{n_1(m_2^2-\mathrm{Re}m_2+c)}$$

$$k_3 = \frac{A-c(k_1+k_2+k_4)}{c},$$

$$k_4 = \frac{k_1c(e^{m_1} - e^{m_3}) + k_2c(e^{-m_2} - e^{m_3}) + A(e^{m_3} - 1)}{c(e^{m_3} - e^{-m_4})}$$

The Nusselt number and the skin friction at the channel plates are obtain as

$$Cf|_{\eta=1} = (k_1m_1e^{m_1} - k_2m_2e^{-m_2} + k_3m_3e^{m_3} - k_4m_4e^{-m_4})e^{-\lambda t}, \quad (18)$$

$$Cf|_{\eta=0} = (k_1m_1 - k_2m_2 + k_3m_3 - k_4m_4)e^{-\lambda t}, \quad (19)$$

$$Nu|_{\eta=1} = -\left(\frac{m_1e^{m_1} - m_2e^{-m_2}}{n_1}\right)e^{-\lambda t}, \quad (20)$$

$$Nu|_{\eta=0} = -\left(\frac{m_1+m_2}{n_1}\right)e^{-\lambda t}, \quad (21)$$

IV. RESULTS AND DISCUSSIONS

The current study emphasizes the behavior of unsteady flow of a viscous, incompressible fluid between two unbounded parallel permeable plates. The systems of momentum and heat transfer equations are solved analytically with the help of variable separable method. The numerical calculation for fluid velocity, fluid temperature, skin friction and Nusselt number has been achieved to analysis the influence of various parameters. Table 1 depicts a comparison between analytical and numerical solutions for the skin friction and Nusselt number using Runge-Kutta-Fehlberg integration scheme. An excellent agreement is achieved; this demonstrates the accuracy of our numerical procedure.

The consequence of different parameters has been discussed with the help of respective graphs. It noteworthy that our analytical results are only valid for cases

Table 1: Comparison between analytical and numerical solution when $\mathrm{Re} = Gr = 0.5, Nr = S = M = A = 0.1, \mathrm{Pr} = 3, \lambda = 1.$

t	$Cf\ (y=0)$ Exact	$Cf\ (y=0)$ Numerical	$Nu\ (y=0)$ Exact	$Nu\ (y=0)$ Numerical
0	0.26656106	0.26656103	3.1492637	3.1492635
0.3	0.19747329	0.19747327	2.3330319	2.3330320
0.7	0.13237030	0.13237031	1.5638780	1.5638781
1.0	0.02665610	0.02665610	0.31492637	0.3149262

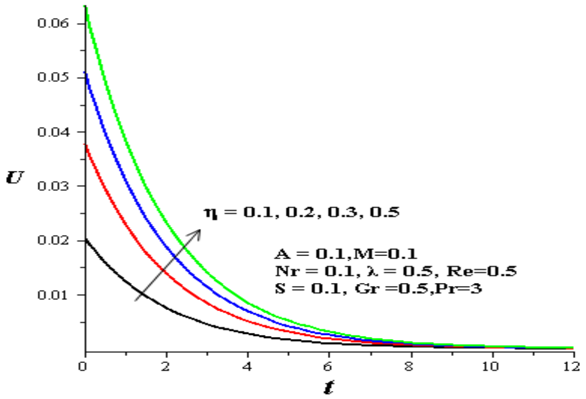

Figure 2: Fluid Velocity for increasing time.

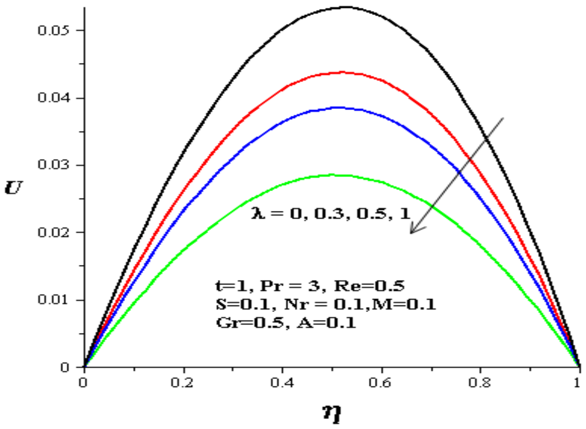

Figure 3: Fluid Velocity for increasing λ.

where $\lambda > 0$ and $\lambda \neq M$. Figure 2 interprets the influence of various values of η against time on the fluid velocity. From the figure, we can conclude that velocity of fluid raises from both left and right walls towards the channel centerline region. However, decay in the velocity has been observed with respect to time at all the point of the channel. Physically speaking, this may be attributed to the interaction of imposed exponential time temperature at the wall with the fluid motion. Figure 3 describes the consequences of wall temperature decay parameter λ on velocity profile at different point of the channel. From figure, it can be noted that increasing value of λ decreases the velocity of fluid due to its decay nature. Generally, the fluid attains it maximum velocity along the channel centerline region while it is minimum with zero axial velocity at the both permeable plates because of the imposed no slip condition. Figure 4, describes influence of suction/injection Reynolds number (Re*)* on fluid velocity profiles. As Re enhances, both the fluid injection into the channel from left plate and fluid suction out of the right plate increase. Interestingly, an enhancement in fluid velocity profiles is observed with increment in suction/in-

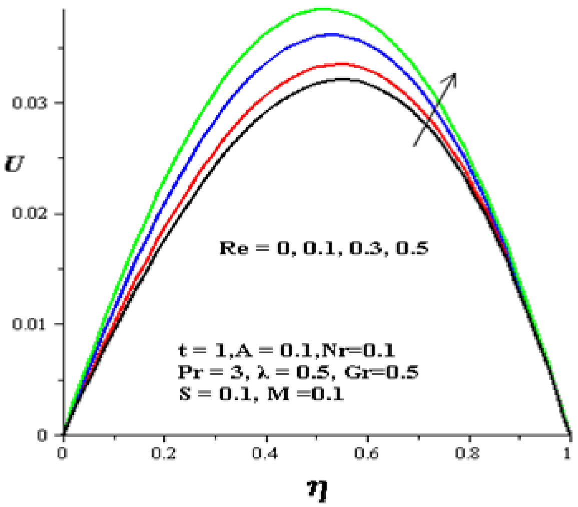

Figure 4: Fluid Velocity for growing Re.

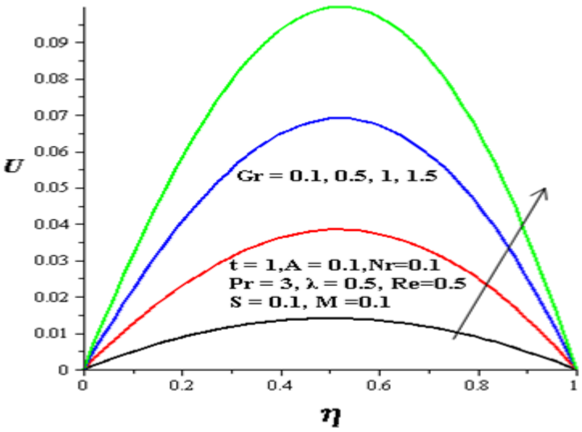

Figure 5: Fluid Velocity for growing Gr.

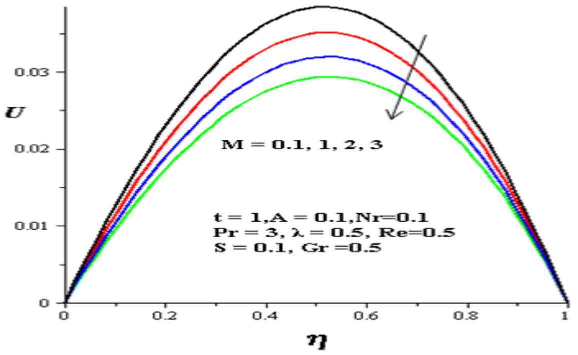

Figure 6: Fluid Velocity for growing M.

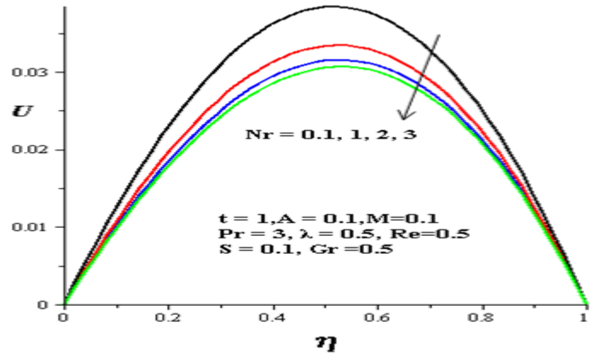

Figure 7: Fluid Velocity for growing Nr.

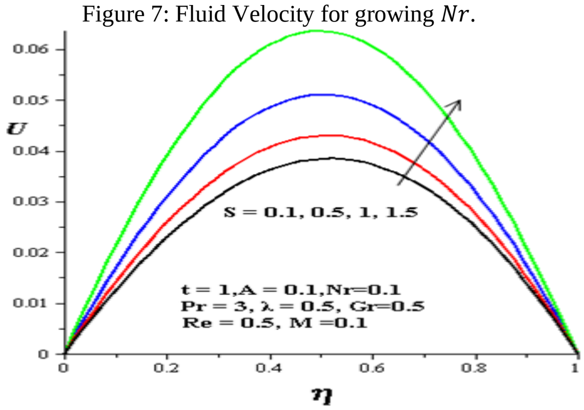

Figure 8: Fluid Velocity for growing S.

jection Reynolds number (Re). The combined effects of increasing injection/suction with the imposed axial pressure gradient leads to improvement in the fluid velocity in the axial direction and towards the right wall. Velocity is high in the middle of the channel while it observed zero at both walls, which satisfies the given boundary conditions. Figure 5 depicts the upshot of the Grashof number Gr on velocity profile at different channel length. The enhanced values of Gr enhance the velocity of fluid which is due to improvement in Gr enhances the buoyancy effects due to temperature difference as a result of wall heating, the fluid becomes lighter and flow faster. It is utmost in the center of the channel while it is least at the both walls for various values of Gr.

Figure 6 indicates the influence of the transversely imposed magnetic field parameter on velocity field within the channel. As M increases, the intensity of magnetic field on the flow is enhanced, consequently, the velocity of fluid diminished because of the opposing effects of Lorentz force to the flow direction. This resistance effect of magnetic field on conducting fluids enhances its usage for flow control mechanism in industrial and engineering setting. Figures 7 and 8 show the impact of heat source parameter S and thermal radiation parameter Nr on velocity field respectively. Increasing Nr reduces the velocity of fluid because of the fact that momentum boundary layer thickness reduces for increased thermal radiation parameter, while heat source parameter S enhances the fluid velocity because of the fact that increasing S enhances the internal heat generation within the fluid because of heat source, consequently, the fluid becomes bright and flow faster. Velocity is utmost in center of the channel for both parameters while it is zero at the both walls which satisfies the given boundary conditions. Figure 9 is plotted to analyze the impact of Prandtl number Pr on velocity profile against the channel width. We utilized the Prandtl number $\mathrm{Pr} = 0.7, 3, 7, 10$ in our numerical simulation. This represents the Pr for water and gases, since the Pr for water ranges from 1 to 10 and that of gases such as water vapour ($\mathrm{Pr} = 0.7$ to 1). From the figure we conclude that that increasing Prandtl number accelerates the fluid velocity. It is because of increasing in Pr decreases the fluid thermal diffusivity and increases the viscous heating effects, this invariably leads to additional heating of the fluid, consequently, the fluid becomes bright and flow faster.

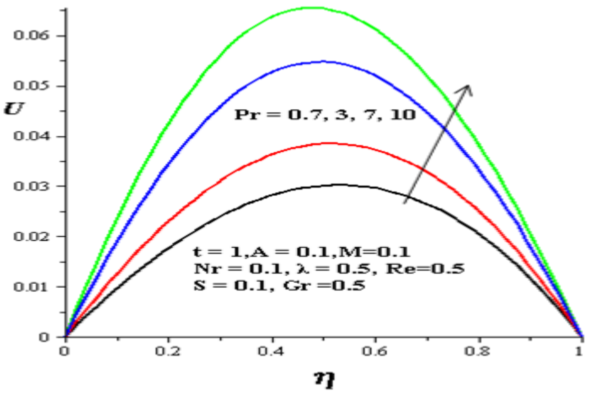

Figure 9: Fluid Velocity for growing Pr.

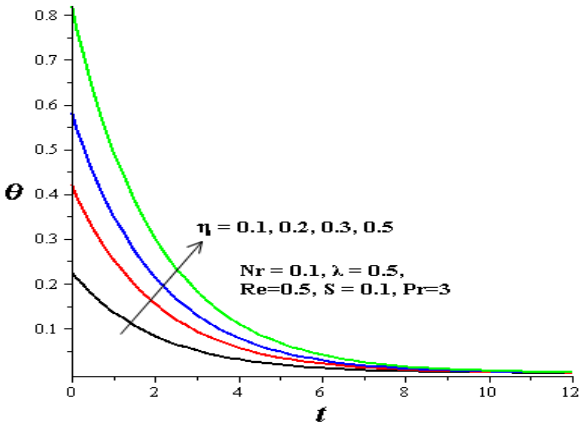

Figure 10: Temperature profiles for increasing time.

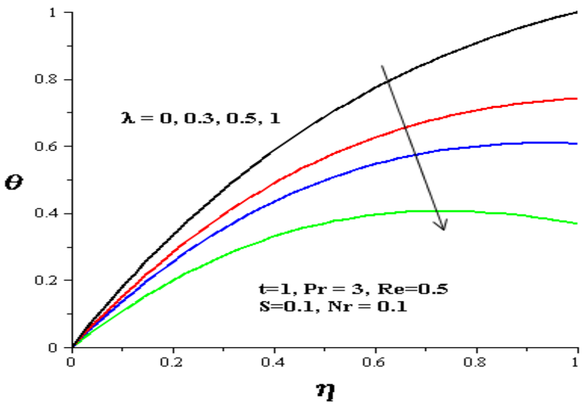

Figure 11: Temperature profiles for increasing λ.

Figure 10 explains the influence of channel width on temperature field at different time. We found that temperature is increasing from left wall towards right wall of the channel, which satisfies our assumption taken into the modeling of the problem. While it is decreasing with increasing time due to term $e^{-\lambda t}$ present in the solution. Figure 11 is sketched for temperature field for numerous values of wall temperature decay parameter against channel width. It is obvious from graph that increasing values of λ reduces the temperature. It is high at right wall comparative to left wall.

Figure 12 describes that increasing Re increases the temperature of fluid keeping higher temperature at right wall. Since increasing Re increases the velocity gradient resulting to growing viscous dissipation as well as an increment in the temperature field due to viscous heating.

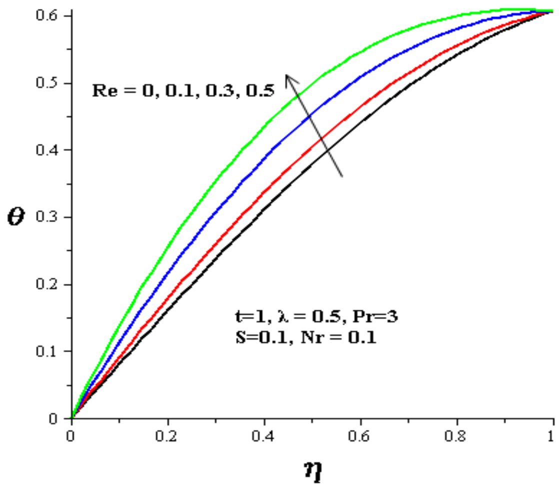

Figure 12: Fluid temperature for growing Re.

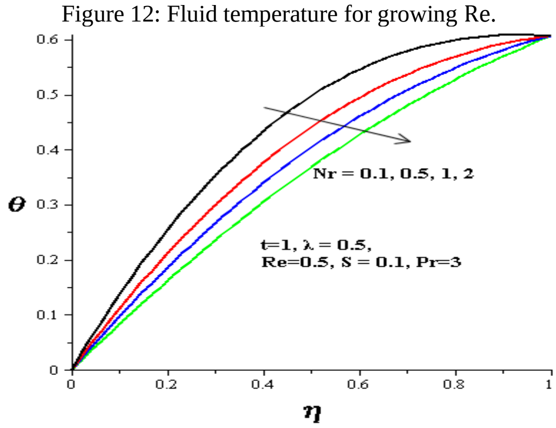

Figure 13: Fluid temperature for growing Nr.

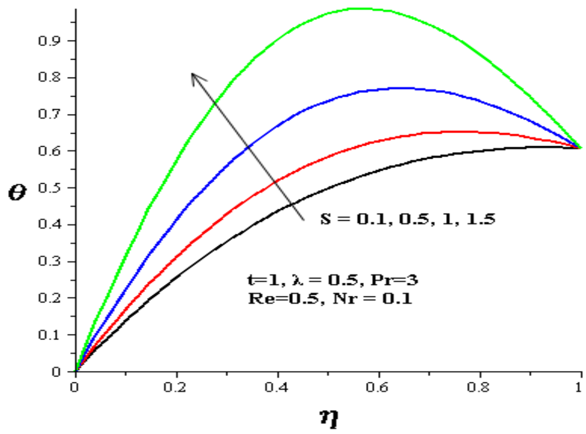

Figure 14: Fluid temperature for growing S.

From Fig. 13, we explain that the increasing thermal radiation parameter lessens the temperature of fluid keeping higher it at right wall. Since increasing Nr increases the radiative heat loss from the fluid and consequently, the temperature reduces. Figure14 shows that increasing heat source parameter S enhances the temperature profile due to fluid internal heat generation due to additional heat source, consequently, the fluid temperature increases. Higher temperature can be observed at right wall of the channel in comparison of left wall. Figure 15 narrate the impact of Prandtl number on temperature profile at different point of channel. From graph we noticed that improving value of Prandtl number increases the tempera-

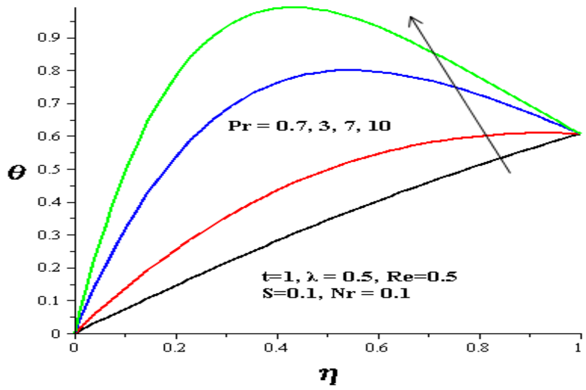

Figure 15: Fluid temperature for growing Pr.

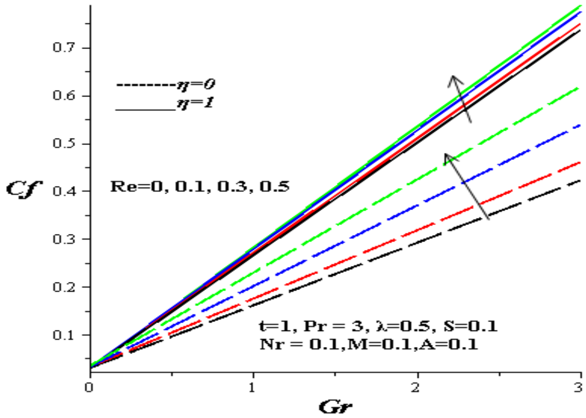

Figure 16: Skin friction for growing Re and Gr.

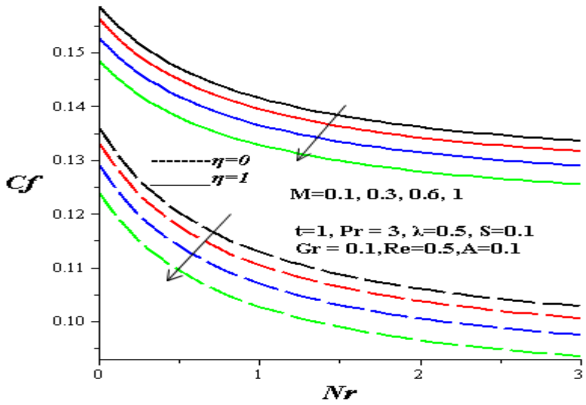

Figure 17: Skin friction for growing M and Nr.

ture profile. Since increasing Pr increases the viscous heating activities within the fluid as compare to that of thermal diffusivity tends to increment in fluid temperature.

Figure 16 delineates the influence of Reynolds number Re on skin friction against Grashof number Gr at both plates of the channel. The enhanced Re and Gr improves the skin friction on both walls. Since, increasing Gr and Re will increase the fluid velocity gradient at the channel plates and as a result the skin friction intensifies. Skin friction is lower at left plate while higher at right plate. Figure 17 represents the skin friction at both wall of the channel for numerous values of M against Nr. Increasing M and Nr decreases the skin friction on both walls. Increasing Nr increases the skin friction on both walls. It is due to increasing M and Nr decreases the fluid velocity

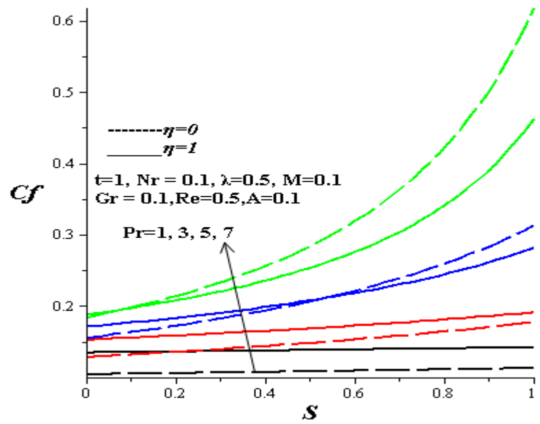

Figure18: Skin friction for increasing Pr and S.

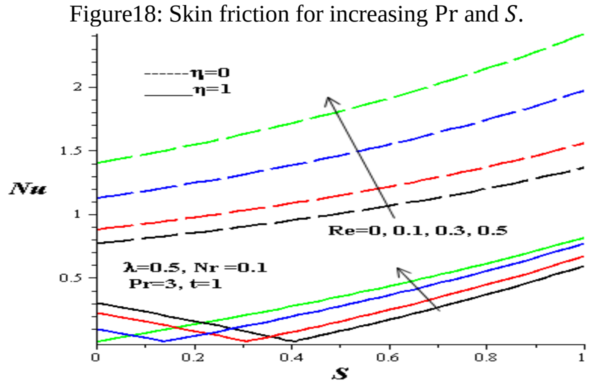

Figure 19: Nusselt number with increasing Re and S.

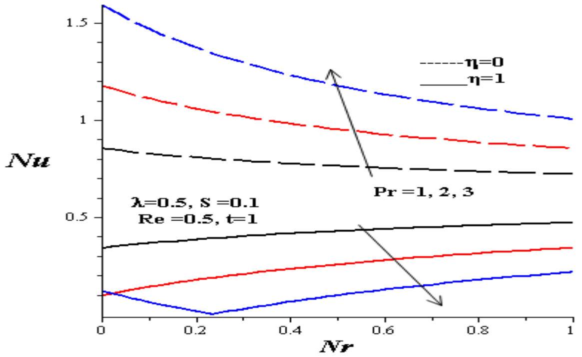

Figure 20: Nusselt number with increment in Pr and Nr.

as well as the velocity gradient at the channel walls and consequently, the skin friction decreases. Figure 18 is plotted for skin friction for growing Pr and heat source parameter S and an increment has been seen in skin friction with increment in the values of S and Pr. Skin friction is observed high at the right plate because of suction effects and low at the left plate because of injection effects.

Figure 19-21 have been plotted for Nusselt numbers at the both channel walls for different parameters. Nusselt number is becoming greater in size with enhanced Re and heat source parameter S at both channel walls. Nusselt number is becoming greater in size with enhanced Prandtl number Pr at left wall while its reverse effect has been seen on right wall. It is decreasing with increasing Nr at left wall while its reverse effect is observed at right wall. Nusselt number is becoming high at left plate comparative to right plate for the same values

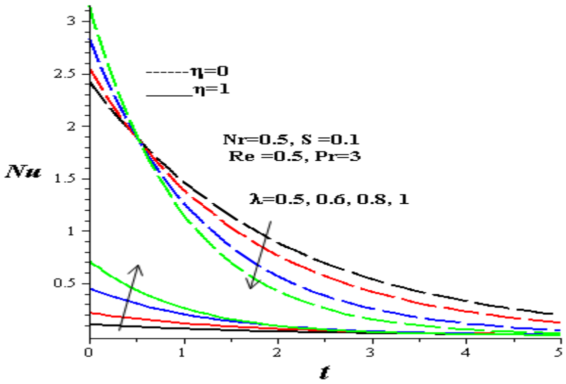

Figure 21: Nusselt number with increment in t and λ.

of temperature decay parameter λ. It reduces at left wall while increases at right plate with increment in λ. Note that increment in λ decreases the fluid temperature at the right wall, this invariably leads to an improvement in the wall heat flux. A slight increase and reduce in Nu at the left wall as λ increases may be ascribed to the coalesced effects of fluid injection and temperature gradient at the left plate. Nu is higher at left plate with low temperature and lower at right wall high temperature due to Fourier heat conduction law.

V. CONCLUSIONS

Transient hydromagnetic flow of conducting fluid through a channel with permeable walls in the presence of buoyancy force and thermal radiation has been discussed. Analytical technique has been applied to solve the problem. We conclude the following remarks on the basis of results:

- Velocity of fluid is utmost at the center of the channel while it is lowest at the both walls.
- Velocity is increasing with increasing values of Re, Pr while its reverse behavior is seen for M, λ, Nr.
- Temperature is increasing from left to right wall of the channel as assumed in the modeling and it is decreasing with increasing t due to nature of its solution.
- Temperature is increasing with Pr while it is decreasing for λ, Nr.
- Skin friction is more at right wall in comparison of left wall.
- Skin friction is becoming greater in size with increasing values of S, while decreasing with increasing values of M, Nr.
- Rate of heat transfer is low at right plate comparative to left plate.

Finally, it is evidence that our results revealed the biomagnetic fluid dynamics and heat transfer characteristics during deep heat muscle treatment physiotherapy scenario where thermal radiation therapy is clinically employed.

NOMENCLATURE

u: Fluid velocity in x-direction.
p: Fluid velocity pressure.
T: Fluid temperature.
σ: Fluid electrical conductivity.
ρ: Fluid density.
υ: Kinematic viscosity.
k: Thermal conductivity coefficient.
c_p: Specific heat at constant pressure.
Q: Gravitational acceleration.
τ: Thermal expansion coefficient.
g: Gravitational force.
β: Heat source parameter.
V: Wall suction / injection velocity.
Pr: Prandtl number.
Re: suction/injection Reynolds number.
Gr: Grashof number.
M: Magnetic field parameter.
S: Heat source parameter.
Nr: Thermal radiation parameter.
λ: Wall temperature decay parameter.
α: Frequency parameter.

REFERENCES

Adhikary, S.D., and Misra, J.C. (2011) Unsteady Two Dimensional Hydromagnetic Flow and Heat Transfer of a Fluid. *International Journal of Applied Mathematics and Mechanics*. **7**, 1-20.

Ansari, S., Seth, G.S., and Nandkeolyar, R. (2011) Unsteady Hartmann flow in a rotating channel with arbitrary conducting walls. *Mathematical and Computer Modelling*. **54**, 765-779.

Attia, H.A., and Aboul-Hassan, A.L. (2003) The effect of variable properties on the unsteady Hartmann flow with heat transfer considering the Hall effect. *Applied Mathematical Modelling*. **27**, 551-563.

Babu, R.S., Kumar, B.R., and Makinde, O.D. (2018) Chemical Reaction and Thermal Radiation Effects on MHD Mixed Convection over a Vertical Plate with Variable Fluid Properties. *Defect and Diffusion Forum*. **387**, 332–342.

Brewster, M.Q. (1992) *Thermal radiative transfer and properties*. John Wiley and sons Inc. New York, USA.

Cramer, K.R., and Pai, S.I. (1973) *Magnetofluid Dynamics for Engineers and Applied Physicists*. McGraw–Hill, New York, USA.

Das, A., Dharodi, V.S. and Tiwari, S.K. (2014) Visco-elastic fluid simulations of coherent structures in strongly coupled dusty plasma medium. *Physics of Plasmas*. **21,** 073705.

Das, S., Jana, R.N., and Makinde, O.D. (2015) Mixed convective magnetohydrodynamic flow in a vertical channel filled with nanofluids. *Engineering Science and Technology an International Journal*. **18**, 244-255.

Gau, C., Yih, K., and Aung, W. (1992) Reversed flow structure and heat transfer measurements for buoyancy-assisted convection in a heated vertical duct. *ASME, J. Heat Transfer*. **114**, 928–935.

Glukhov, A.F. and Sidorov, S.S. (2019) Periodic convective processes in a magnetic fluid in vertical channels. *Fluid Dynamics*. **54**, 451–456.

Govindarajan, R., and Sahu, K. C. (2011) Linear stability of double-diffusive two-fluid channel flow. *Journal of Fluid mechanics*. **687**, 529-539.

Hartmann, J., and Lazarus, F. (1937) The influence of a transverse uniform magnetic field on the flow of a conducting fluid between two infinite parallel, Stationary, and Insulated Plates. *K. Dan. Vidensk. Selsk. Mat. Fys. Medd.* **15**, 346-369.

Hussam, W.K., and Sheard, G.J. (2013) Heat transfer in a high Hartmann number MHD duct flow with a circular cylinder placed near the heated side-wall. *International Journal of Heat and Mass Transfer*. **67**, 944-954.

Khan, O.U., Hoffmann, K.A., Dietiker, J.F. (2007) Validity of low magnetic Reynolds number formulation of magnetofluiddynamics. *38th AIAA Plasmadynamics and Lasers Conference In conjunction with the 16th International Conference on MHD Energy Conversion*, Miami, 4374.

Makinde, O.D., and Chinyoka, T. (2010) Numerical investigation of transient heat transfer to hydromagnetic channel flow with radiative heat and convective cooling. *Communications in Nonlinear Science and Numerical Simulations*. **15**, 3919-3930.

Makinde, O.D. and Ogulu, A. (2008) The effect of thermal radiation on the heat and mass transfer flow of a variable viscosity fluid past a vertical porous plate permeated by a transverse magnetic field. *Chemical Engineering Communications.* **195**, 1575-1584.

Makinde, O.D. and Onyejekwe, O. (2011) A numerical study of MHD generalized Couette flow and heat transfer with variable viscosity and electrical conductivity. *Journal of Magnetism and Magnetic Materials*. **323**, 2757-2763.

Malton, M., and Schweitzer, S. (1974) Viscous MFD low Hartmann flow in an annular gap—a magnetic Prandtl number expansion. *Journal of the Franklin Institute*. **297**, 259-285.

Nadler, S.F., Weingand, K., and Kruse, R.J. (2004) The physiologic basis and clinical applications of cryotherapy and thermotherapy for the pain practitioner. *Pain Physician*. **7,** 395-399.

Ozisik, M.N. (1973) *Radiation Transfer and Interactions with Conduction and Convection*. Wiley-Inter-science Publication, USA.

Pandey, A.K. and Kumar, M. (2016) Effect of viscous dissipation and suction/injection on MHD nanofluid flow over a wedge with porous medium and slip. *Alexandria Engineering Journal*, **55**, 3115-3123.

Pandey, A.K. and Kumar, M. (2017) Natural convection and thermal radiation influence on nanofluid flow over a stretching cylinder in a porous medium with viscous dissipation, *Alexandria Engineering Journal*. **56**, 55-62.

Prakash, J. and Makinde, O.D. (2011) Radiative heat transfer to blood flow through a stenotic artery in the presence of erythrocytes and magnetic field. *Latin American Applied Research*. **41**, 273-277.

Prakash, O., Makinde, O.D., Singh, S.P., Jain, N. and Kumar, D. (2015a) Effects of stenosis on non-Newtonian flow of blood in blood vessels. *International Journal of Biomathematics*. **8**, 1550010.

Prakash, O., Makinde, O.D., Kumar, D. and Dwivedi, Y.K. (2015b) Heat transfer to MHD oscillatory dusty fluid flow in a channel filled with a porous medium. *Sadhana- Academy Proceedings in Engineering Science*. **40**, 1273-1282.

Prakash, O., Makinde, O.D. and Monaledi, R.L. (2020) Unsteady MHD flow of radiating Casson fluid through a permeable channel with slip, buoyancy force and heat source. *Latin American Applied Research.* **50,** 315-320.

Ramakrishnan, K., and Shailendhra, K. (2013) Hydromagnetic blood flow through a uniform channel with permeable walls covered by porous media of finite thickness. *Journal of Applied Fluid Mechanics*. **6**, 39-47.

Ramamurthy, G., and Shanker, B. (1994) Magnetohydrodynamic Effects on Blood Flow through Porous Channel. *Medical and Biological Engineering and Computing*. **32**, 655-659.

Rosseland, S. (1936) *Theoretical astrophysics*. Oxford University, New York, NY, USA.

Sarris, I.E., Zikos, G.K., Grecos, A.P., and Vlachos, N.S. (2006) On the limits of validity of the low magnetic Reynolds numbers approximation in MHD natural-Convection heat transfer. *Numerical Heat Transfer. Part B*, **50**, 157-180.

Tzirtzilakis, E.E. (2005) A mathematical model for blood flow in magnetic field. *Physics of Fluids*. 17, 1-15.

Upreti, H., Pandey, A.K. and Kumar, M. (2018) MHD flow of Ag-water nanofluid over a flat porous plate with viscous-Ohmic dissipation, suction/injection and heat generation/ absorption. *Alexandria Engineering Journal*. **57**, 1839-1847.

Upreti, H., Pandey, A.K. and Kumar, M. (2020a) Thermophoresis and suction/injection roles on free convective MHD flow of Ag–kerosene oil nanofluid. *Journal of Computational Design and Engineering*. **7**, 386–396.

Upreti, H., Pandey, A.K., Kumar, M. and Makinde, O.D. (2020b) Makinde, Ohmic Heating and Non-uniform Heat Source/Sink Roles on 3D Darcy–Forchheimer Flow of CNTs Nanofluids Over a Stretching Surface. *Arabian Journal for Science and Engineering*. **45**, 7705–7717.

Yang, H.K., and Yu, C.P. (1974) Combined forced and free convection MHD channel flow in entrance region. *International Journal of Heat and Mass Transfer*. **17,** 681-691.

Zamzari, F., Mehrez, Z. and Cafsi, A.E. (2019) Heat transfer enhancement of pulsating flow in an Open cavity subjected to uniform magnetic field. *Fluid Dynamics*. **54**, 428–438.

Received: September 32, 2020
Sent to Subject Editor: October 22, 2020
Accepted: July 12, 2021
Recommended by Subject Editor Fabio Giannetti